Applied Surface Science 646 (2024) 158943

Contents lists available at ScienceDirect

Applied Surface Science

journal homepage: www.elsevier.com/locate/apsusc

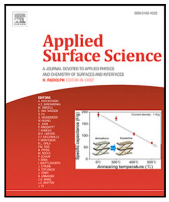

Full length article

Tailoring single-molecule conductance with structured graphene electrodes

Joel G. Fallaque [a,b,*], Sandra Rodríguez-González [b,c], Cristina Díaz [b,d], Fernando Martín [a,b,e]

[a] Instituto Madrileño de Estudios Avanzados en Nanociencia (IMDEA-Nano), Campus de Cantoblanco, 28049, Madrid, Spain
[b] Departamento de Química, Módulo 13, Universidad Autónoma de Madrid, 28049, Madrid, Spain
[c] Departamento de Química Física Aplicada, Módulo 14, Universidad Autónoma de Madrid, 28049, Madrid, Spain
[d] Departamento de Química Física, Facultad de Ciencias Químicas, Universidad Complutense de Madrid, 28040, Madrid, Spain
[e] Condensed Matter Physics Center (IFIMAC), Universidad Autónoma de Madrid, 28049, Madrid, Spain

ARTICLE INFO

MSC:
0000
1111

Keywords:
Single-molecule junction
Moiré pattern
Current
Transport properties
Electronic structure

ABSTRACT

Modulation of electric currents through single-molecule junctions is usually achieved by synthesis of molecules with desired functionalities, in conjunction with suitable molecule–electrode contacts through specific anchoring groups. An alternative to this approach, barely explored so far, is to use structured electrodes, where conductivity could eventually be controlled by changing the specific anchoring site within the very same electrode. Here, we theoretically investigate how to exploit the pronounced anisotropy of corrugated graphene deposited on Ru(0001) (Gr/Ru) to tailor single-molecule conductivity in 4-aminophenyl and 4-aminobenzonitrile. We show that currents induced in the upper and lower anchoring positions in the Gr/Ru moiré are substantially different, irrespective of the chosen molecule. The magnitude of these currents can differ by as much as an order of magnitude at specific bias voltages. We also show that both molecules display rectifying properties, which can differ by up to a factor of five in different anchoring sites. Interestingly, the observed modulations strongly depend on the chemical binding nature between the molecule and the electrode, (strong) covalent bond for 4-aminophenyl and (weak) physisorption for 4-aminobenzonitrile. All this suggests that Gr/Ru can be an ideal electrode to modulate single-molecule electric conductivity under experimental conditions that are available in many laboratories.

1. Introduction

Since the first evidence showing that conjugated oligomers can become active parts of electronic devices [1], molecular electronic junctions have emerged as potential candidates for new technological applications in the context of moletronics [2,3]. The blossoming of these technologies relies on our ability to design and tune the electronic properties of the junctions at will. Fine-tuning of molecule-junction properties can be achieved by synthesizing molecules with desired functionalities, in conjunction with the design of suitable molecule–electrode contacts through specific anchoring groups. To disentangle the individual effect of these three components (molecule, anchoring group, and electrode) on the junctions, systematic investigations should ideally be performed by fixing two components and varying the third one. This can be done, e.g., by performing single-molecule break-junction experiments in which the molecule is placed in between a scanning tunneling microscope (STM) tip (top electrode) and an extended conducting solid substrate (bottom electrode) [4].

Many previous studies have sought to exploit the chemical properties of molecules [5–7]. For example, aromatic molecules display in general much lower junction tunneling-barrier heights, hence higher conductivity, than aliphatic molecules [8]. This is because the energies of the molecular orbitals of the former molecules are more closely aligned with the Fermi level of the electrodes. Conduction depends also very much on the tunnel junction length [9–14]. Thus, chemical design of molecules with the appropriate electronic structure and length is widely used to modulate conductivity through junctions. But this is not always possible, e.g., when pinning effects are at play [15].

The second component, anchoring groups, which are necessary to effectively bind the molecules to the electrodes in specific positions, are far from being passive actors. They modulate the effective overlap between the electronic wave functions of the molecule and the electrodes, thus affecting the conductivity [16]. For example, molecules containing thiol (-SH) and pyridyl (-PY) groups have been shown to form stronger bonds with Au electrodes than carboxylic-acid (-COOH), amine (-NH_2), isocyano (-CN) and, isothiocyanate (-SCN) groups [17,18], leading to more stable molecular junctions even under ambient conditions [17], but, more importantly, allowing for a high variability of conductance values [11,19]. Changing the anchoring positions can also significantly

* Corresponding author at: Departamento de Química, Módulo 13, Universidad Autónoma de Madrid, 28049, Madrid, Spain.
E-mail address: joel.fallaque@uam.es (J.G. Fallaque).

https://doi.org/10.1016/j.apsusc.2023.158943
Received 6 September 2023; Received in revised form 27 October 2023; Accepted 16 November 2023
Available online 19 November 2023

modify the conductivity [20]. Importantly, the anchoring groups may also ensure the stability of the junction with increasing length of the molecule, as shown, e.g., for oligoyne molecular wires [12]. These effects are even more pronounced for non-metal electrodes [21,22].

Concerning the third component of the junctions, the electrodes, the most popular ones are made of metals [7]. Group 10 metals, Pd, Ni and Pt, have been shown to promote more efficient electronic transport than group 11 metals, such as Au, Ag, and Cu, due to their stronger d-orbital nature and their larger local density of states near the Fermi level [16,23–26]. Among group 11 metals, conductance has been shown to be higher for Au than for Ag electrodes [24,26,27], though the latter turn out to be more stable in hydrogen environment [28]. Despite the diverse scenarios provided by metal electrodes, they are also affected by some limitations. For example, they may present stability problems due to the high mobility of the surface atoms. Also, controlling the metal-to-molecule interface at the nanoscale is very difficult, which hampers reproducibility. In contrast, graphite or graphene-based bottom electrodes are more stable [29–31]. They can also enhance conductivity [32–34] and may even moderate its exponential decay at the junction sites [13,14]. Furthermore, this type of molecular junctions show controllable rectification properties [31,35,36] due to the asymmetry in the coupling to the electrodes.

An alternative to traditional electrodes, so far barely explored, is provided by stable structured electrodes, where conductivity is expected to depend on the anchoring site in the electrode. In this case, identical molecules placed on different sites may exhibit different conductivity, all without the need for changing the molecule's structure and/or functionalization, nor the nature of the electrode. To enhance stability, such an electrode should ideally have a graphene-like character, but should also incorporate the necessary structural modifications to allow for site-selective conductivity. Materials that satisfy these requirements are those formed by a graphene layer absorbed on a metal substrate [37]. Even when adsorbed on a metal, graphene preserves the main properties that make it ideal for electrode manufacturing, such as the low atom mobility, weak interfacial dipole, and a large number of anchoring positions at room temperature through strong C–C molecule–electrode bonds [38] or van der Waals molecule–electrode interactions that preserve the molecular geometry [39,40]. Previous studies have focused on electrodes where graphene is weakly bound to the metal, so that its electronic properties remain almost intact all over the surface, thus preventing site-selective conductivity. For example, in this context, graphene has been tested as protective layer for Au electrodes [41] resulting in a drastic reduction of the conductance with respect to a bare Au electrode irrespective of the anchoring group and the molecule considered. Also, graphene adsorbed on copper has been used as bottom electrode to study molecular electronics on self-assembled monolayers of alkylamines [42]. These junctions are electrically stable in ambient conditions and their electrical properties have been found to be similar to those of junctions formed with pure Au and Ag electrodes.

In contrast, graphene adsorbed on Ru(0001) (thereafter Gr/Ru) displays a versatility that can be exploited to tune the electronic transport properties in the junction just by changing the anchoring position of the molecule in the electrode. Indeed, due to the lattice mismatch, upon adsorption on Ru(0001), graphene adopts a pronounced and strongly corrugated (> 1 Å) moiré superstructure [43–45] characterized by the presence of well-defined physisorption and chemisorption domains [46]. These domains correspond, respectively, to the upper and lower regions of the moiré. This strong structural modulation of graphene is accompanied by a similarly strong spatial modulation of its electronic properties [47], which reflects in the localized nature of the electronic states close to the Fermi level in the upper regions and above the Fermi level in the lower regions. These properties have been and are currently exploited in many laboratories to selectively bind molecules in specific sites [37], to catalyze chemical reactions in different regions of the moiré [48], to generate single-molecule magnetic impurities [49,50] or to build long-range magnetic order in self-assembled monolayers of organic molecules [51], to name a few examples.

In this work, we theoretically investigate how to exploit these unique electronic properties of Gr/Ru to tailor single-molecule conductivity in 4-aminophenyl and 4-aminobenzonitrile by varying their anchoring positions on a bottom Gr/Ru electrode in the presence of a Ru STM tip. We have chosen these molecules because of the different nature of the chemical bonding with the substrate. 4-aminophenyl has a radical character, so that it is prone to covalently bind to the substrate. This molecule has been synthesized by Rudnev at al [31] and Tehrani et al. [52] by means of electrochemical grafting of 4-nitrobenzenediazonium salts and subsequent electrochemical reduction of the nitro groups to amine. Using a similar approach, Ambrosio et al. [53] have shown that this is also possible for closely related aminophenyl compounds. In all three experiments, the synthesized molecules form covalent bonds with a graphite substrate, so that one can also expect to do so with Gr/Ru. In contrast, 4-aminobenzonitrile cannot make a covalent bond with the substrate. This is supported by previous experiments showing that molecules containing an additional CN group can only physisorb on Gr/Ru (see, for instance, [49,51]. Thus, in this case, the Ru tip must be used to pull the molecule from the bottom electrode. We have performed state-of-the-art fully atomistic density functional theory (DFT) and transport calculations in the Gr/Ru-molecule-Tip(Ru) junctions for bias voltages between −2 and +2 V. We have found very different values of the induced currents when comparing upper and lower anchoring positions in the Gr/Ru moiré, irrespective of the chosen molecule. These values can differ by more than an order of magnitude at specific bias voltages. Furthermore, the difference can be modulated at will by just varying such bias. Interestingly, for bias where differences in the electric current are more pronounced, 4-aminophenyl and 4-aminobenzonitrile behave quite differently: for 4-aminobenzonitrile, the largest current values are obtained for molecules anchored on the lower areas of the moiré, while for 4-aminophenyl the largest value is obtained on the intermediate areas. These results prove that Gr/Ru is indeed a very promising system to tailor single-molecule electric conductivity under experimental conditions that are rather standard in nowadays laboratories.

2. Theoretical methods

2.1. Construction of the junctions geometries

To evaluate the conductance as a function of the anchoring positions on the Gr/Ru bottom electrode (Fig. 1c), we have considered a graphene monolayer epitaxially grown on a 3-layer Ru(0001) slab. Following Refs. [46,47], the moiré pattern distinctive of this potential electrode has been represented by a 11 × 11 graphene supercell on a 10 × 10 Ru supercell -the lattice parameters of Gr and Ru are 2.46 Å and 2.70 Å, respectively. First, we have performed a geometry optimization of the system by means of density functional theory (DFT) within the generalized gradient approximation (GGA) as implemented in the plane-wave based licensed-code VASP [54]. In applying the GGA, we have used the PBE functional [55] including van der Waals corrections as proposed by Tkatchenko and Sheffler [56]. In all calculations, the projector augmented wave (PAW) method [57] has been used to describe the interaction between the core electrons and the nuclei. The cut-off energy of the plane-wave basis was set at 400 eV, and the optimizations have been computed at the Γ point in the reciprocal space until the forces acting on the atoms were less than 0.01 eV/Å. Geometry optimization of the Gr/Ru bottom electrode has been carried out by fixing the two bottom Ru layers allowing the outermost Ru layer and the Gr to relax. The upper electrode, formed by a 4-atoms pyramidal tip and 3 layers of Ru(0001), has been optimized relaxing only the tip and the outermost layer, using the same convergence

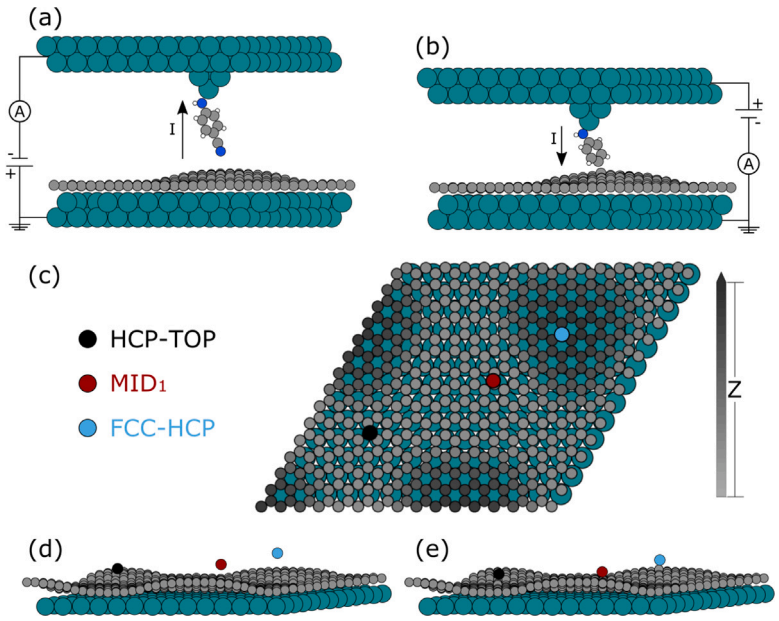

Fig. 1. Optimized geometries for tip-molecule-graphene surface arrangements with (a) 4−aminobenzonitrile and (b) 4−aminophenyl molecules at FCC- HCP position scheming forward and reverse current, respectively. (c): Top view of the positions under study: HCP-TOP (black circle), MID_1 (red circle) and FCC-HCP (light blue circle). (d) and (e): Side view of the positions shown in (c), using 4−aminobenzonitrile and 4−aminophenyl, respectively.

Table 1
Optimized junction distances between the closest atoms of one electrode (tip or graphene) and the molecule. Binding/Adsorption energies in eV of both molecules on top of the Gr/Ru surface.

System	Site	Aniline - d (Å)		4-Aminobenzonitrile - d (Å)	
		Ru_{tip}−$N_{molecule}$	$C_{molecule}$−$C_{graphene}$	Ru_{tip}−$N_{molecule}$	$N_{molecule}$−$C_{graphene}$
Tip-Molecule	–	2.21	–	2.24	–
Graphene-Molecule	HCP-TOP	–	1.57	–	2.88
	MID_1	–	1.57	–	3.28
	FCC-HCP	–	1.57	–	3.04
Tip-Molecule-Graphene	HCP-TOP	2.21	1.56	2.26	3.02
	MID_1	2.17	1.57	2.21	3.29
	FCC-HCP	2.21	1.56	2.23	3.08
System	Site	Binding/Adsorption energy (eV)			
		Aniline		4-Aminobenzonitrile	
Molecule−Gr/Ru	HCP-TOP	−3.15		−0.52	
	MID_1	−1.80		−0.42	
	FCC-HCP	−1.25		−0.15	

criteria as for the bottom electrode. The optimization of the molecule adsorbed on the Gr/Ru electrode has been accomplished allowing the Gr and the molecule to relax, whereas the 3 layers of Ru are kept fixed. In this case, the convergence criterium has been set to 0.05 eV/Åfor the forces acting on the atoms. We have also optimized the subsystem formed by the top-electrode and the molecule, allowing for relaxation of the tip and the molecule's atoms. From these calculations, we obtained the optimized junction distances shown in Table 1 -see *Tip-Molecule* and *Graphene-Molecule* entries. Finally, we have constructed and re-optimized the full junction geometry starting from the previously optimized distances, by simultaneously relaxing the positions of all atoms in the molecule, the graphene atoms, the topmost-layer atoms of Ru and the tip, using 0.05 eV/Åas atomic force limit. The optimized distances are also given in Table 1 -see *Tip-Molecule-Graphene* entry.

2.2. Transmission calculations

Using the above optimized geometries, we have computed the transmissions functions using the TRANSIESTA/TBTRANS packages [58]. TBTRANS is used as a post-processing procedure and is needed to calculate the transmission and current-intensity (I–V) curves from the TRANSIESTA output. In these calculations, we first set the full system by adding 4 more layers of Ru(0001) to the bottom-electrode and 2 more Ru layers to the top-electrode, as a good compromise between accuracy and computational effort. Then, we have performed a single-point calculation using the TRANSIESTA methodology employing 4-layer Ru bulk in both sites, from the full system, as semi-infinite electrodes. As in the previous DFT optimization calculations, the PBE [55] exchange–correlation functional has been used. A single-ζ polarization basis set has been used to describe the valance electrons of Ru atoms and a double-ζ polarization for all the rest. In all cases, we have used a mesh cutoff energy of 200 Ry. The first Brillouin zone has been described using a $2 \times 2 \times 1$ k-mesh, and the core electrons-nuclei interaction by means of norm-conserving pseudopotentials. After obtaining the Hamiltonian, we have computed the transmission functions with TBTRANS using a $8 \times 8 \times 1$ k-mesh. We have also computed the transmission functions under non-equilibrium conditions. To do so, we have performed TRANSIESTA calculations increasing (decreasing) the bias by 0.5 V from 0 V until 2.0 (−2.0) V was reached. Once all Hamiltonian matrices were obtained, we performed spline interpolations within the TBTRANS code to obtain transmission functions at biases $\in$ [−2.0 V; 2.0 V] with δV = 0.1 V. Additionally, TBTRANS integrates the transmission function in the momentum space ($\boldsymbol{k}$-space)

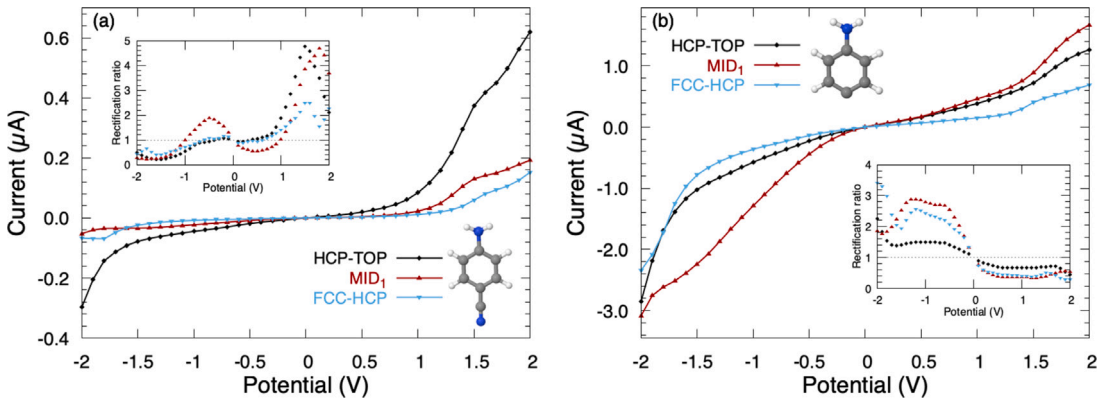

Fig. 2. Current as a function of the applied bias at different anchoring positions (see Fig. 1) for (a) 4−aminobenzonitrile and (b) 4-aminophenyl. In both cases the current is measured from the Gr/Ru surface to the tip. The inset shows the rectification ratio (RR), i.e., $I_{forward}/I_{reversed}$, where at positive biases forward current flows from Gr/Ru to the tip, while the opposite occurs at negative biases.

from bottom to top electrodes, $\mathcal{T}_{BT}$, to obtain the electrical current, I_{BT}, as [58]:

$$I_{BT} = \frac{G_0}{2|e|}\int\int_{BZ} d\boldsymbol{k}d\varepsilon\ \mathcal{T}_{BT,\boldsymbol{k}}(\varepsilon)[n_{F,T} - n_{F,B}], \quad (1)$$

where $G_0 = 2e^2/h$ is the quantum conductance and $n_{F,B/T}$ stands for the Fermi distribution associated to the chemical potential, μ, and the temperature, k_BT, correspond to the electrode B/T. Analogous expressions have been used for current flow from the top electrode to the bottom one, I_{TB}.

3. Results and discussion

For both, 4-aminophenyl and 4-aminobenzonitrile, we have considered 3 different anchoring sites on the moiré pattern. HCP-TOP, MID_1 and FCC-HCP (see Fig. 1), corresponding to the lower, intermediate and higher regions of the moiré, respectively. As previously mentioned, 4-aminophenyl forms a covalent C–C bond with the bottom electrode. Our analysis of the adsorption properties of this system reveals adsorption energies between −1.25 eV, for the FCC-HCP site, and −3.15 eV for the HCP-TOP site, and a $C_{molecule}$ - $C_{graphene}$ distance of 1.57 Å, for the three sites (see Table 1). These values are consistent with those expected for chemisorption. On the other hand, the computed adsorption properties for 4-aminobenzonitrile on Gr/Ru are compatible with physisorption: adsorption energies range between −0.15 eV (FCC-HCP) and −0.52 eV (HCP-TOP), and the $N_{molecule}$-$C_{Graphene}$ distance between 3.28 Å (MID_1) and 2.88 Å (HCP-TOP), as shown in Table 1.

Fig. 2 shows the calculated current flows on these sites at the non-equilibrium regime considering an addition of a chemical shift equal to $V/2$ and $-V/2$ to the Gr/Ru bottom-electrode and tip electrode, respectively, where $V \in [-2.0\ V; 2.0\ V]$ is the potential. Thus, at positive biases (see Fig. 1a), the current flows from the Gr/Ru bottom-electrode to the tip, while, at negative biases (see Fig. 1b), the other way around.

As can be seen, irrespective of the chosen molecule, the calculated currents strongly depend on the anchoring position and can differ by more than an order of magnitude at specific bias voltages. For 4-aminobenzonitrile, the largest values are obtained at positive biases, while, for 4-aminophenyl, they show up at negative biases. For 4-aminobenzonitrile and positive bias voltages, the values of the current at the lower areas of the moiré (HCP-TOP, black curve in Fig. 2a) are much larger than those at the intermediate and higher areas (MID_1 and FCC-HCP). Similarly large differences in the current can be observed for 4-aminophenyl at negative bias, although in this case the largest absolute values correspond to the intermediate area of the moiré (MID_1, red curve in Fig. 2b). As we will show below, this pronounced site-dependent conductivity is the consequence of the very different electronic structure of Gr/Ru on the different areas of the moiré. Importantly, these results suggest that the ability of Gr/Ru to strongly modulate the currents does not seem to depend on the nature of the binding between the molecule and the Gr/Ru electrode (strong covalent binding for 4-aminophenyl and weak dispersive binding for 4-aminobenzonitrile). However, the specific type of modulation does depend on the particular molecule and binding properties.

Interestingly, the I-V curve exhibits a pronounced asymmetry for both molecules, pointing to a rectifier behavior. The insets in Fig. 2 show the corresponding rectification ratios (RR). As can be seen, these ratios depend on the bias polarity. As the currents themselves, the RRs depend very much on the anchoring sites for both molecules. For the FCC-HCP and HCP-TOP anchoring sites, 4-aminobenzonitrile barely shows any rectification between ∼-1 and ∼+1 V, i.e. RR≈1. Thus, for $|V| < 1$V, the current can flow equally well in both directions. Elsewhere, the RR oscillates around 1. For the MID_1 anchoring position, the RR oscillates in the whole range of bias voltages. For all sites, the RR reaches the largest values (up to 5 for the HCP-TOP and MID_1 sites) at $V \geq 1$ V, meaning that in this region the current from the Gr/Ru surface to the tip flows much more easily than in the opposite direction. This effect, called “asymmetric differential resistance”[59–61], is due to the asymmetry and orbitals alignments of the molecules coupled to both contacts (see below). For 4-aminophenyl (Fig. 2b), the RR is significantly different from 1 over the whole range of bias voltages (except, obviously, at zero voltage). In this case, the largest RRs appear at $V \leq -0.5$ V for all 3 anchoring positions, i.e., the current from the tip to the Gr/Ru surface is favored. However, as in the case of the 4-aminobenzonitrile molecule, aniline also exhibits a strong modulation of the RRs with the anchoring site, being approximately 5 times larger in the FCC-HCP and MID_1 sites than in the HCP-TOP site.

To understand the origin of the pronounced site-dependence of the calculated currents and RRs, as well as the different nature of the chemical binding of 4-aminophenyl and 4-aminobenzonitrile with the electrodes, it is useful to look at the corresponding transmission (Fig. 3) and eigenchannel (Fig. 4) functions at zero bias. Fig. 3 displays the transmission functions, $\mathcal{T}(\varepsilon)$, as functions of energy for both molecules. One can see that the transmission values are systematically higher for 4-aminophenyl than for 4-aminobenzonitrile. This is a consequence of the covalent bond between 4-aminophenyl and Gr/Ru, which implies higher hybridization of the molecule and surface states, thus leading to new energy levels and hence enhancing the tunneling mechanism. This statement is further supported by the shape of the eigenchannels at the HOMO and LUMO positions, as well as at -0.5 eV, shown in Fig. 4. As can be seen, orbitals at the molecule-Gr/Ru interaction region are more delocalized in the Gr/Ru-4-aminophenyl-Ru system, as expected for covalent bonding (see also Figs. S1–S4 of the SI). For 4-aminobenzonitrile (Fig. 3a), the largest peaks, associated with transmission through the HOMO and LUMO orbitals of the molecule, lie

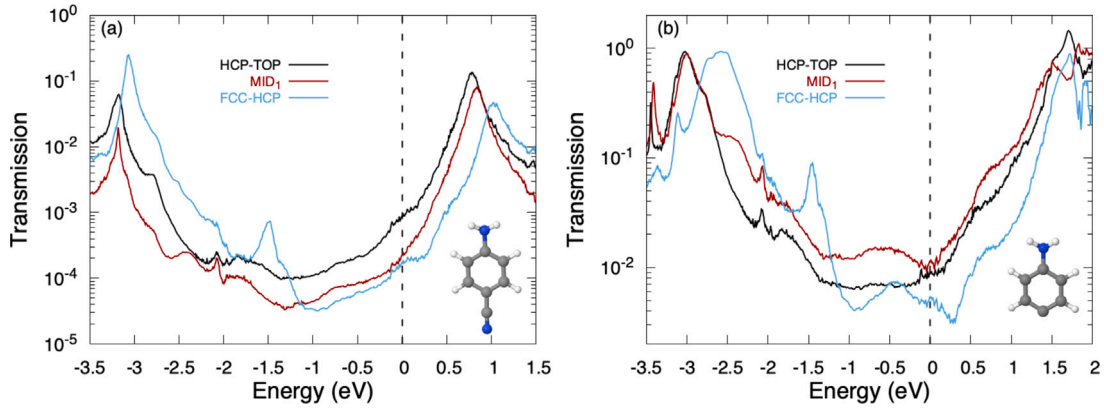

Fig. 3. Transmission functions at the different positions anchoring positions (see Fig. 1) for (a) 4-aminobenzonitrile and (b) 4-aminophenyl. Dashed black lines indicate to the Fermi level.

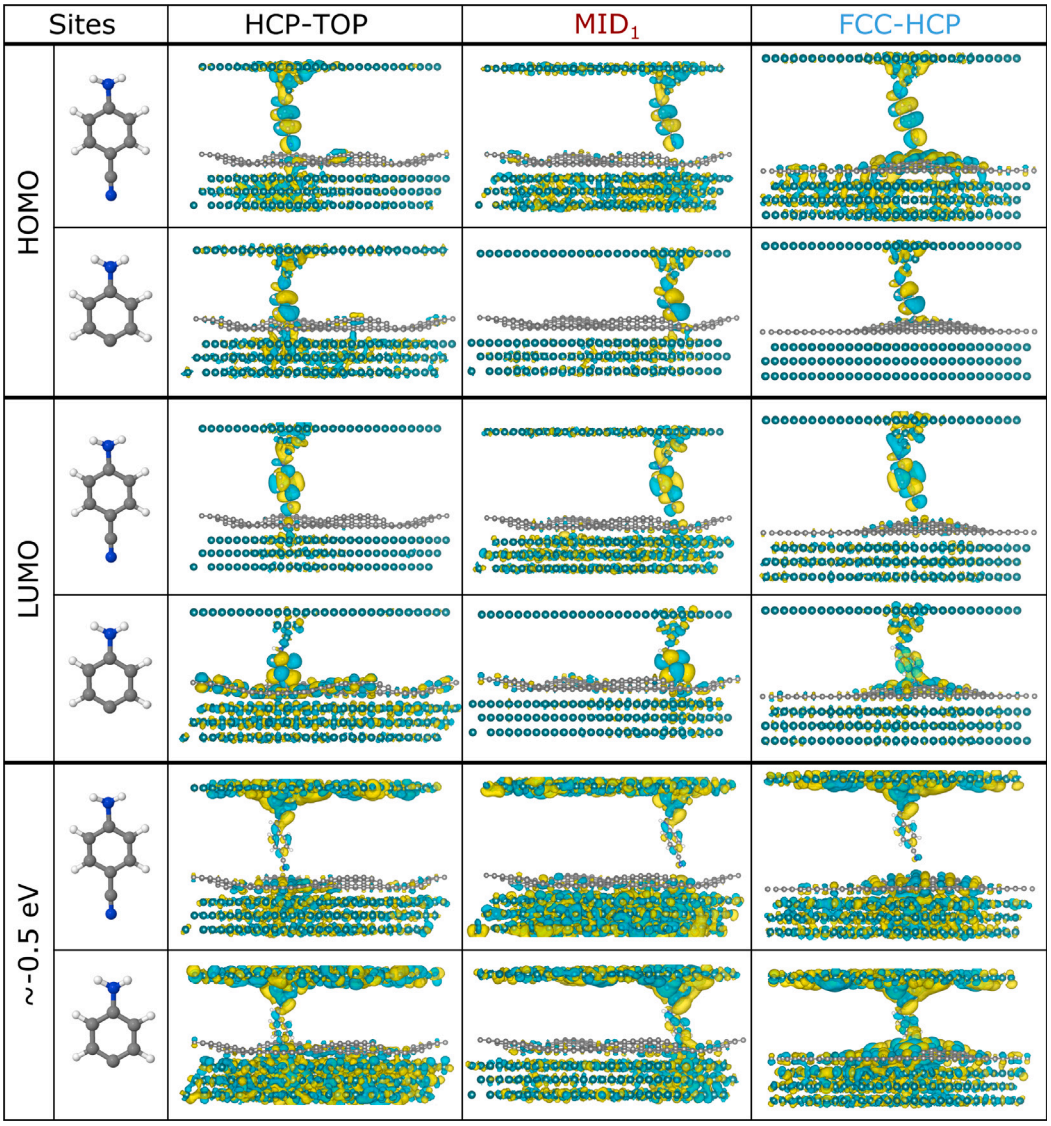

Fig. 4. Eigenchannels at the HOMO (top row, isovalue=0.05) and LUMO (middle row, isovalue=0.05) positions and at ~ 0.5 eV (bottom row, isovalue=0.02) for 4–aminobenzonitrile and 4-aminophenyl. Energy levels obtained from Fig. 3. For simplicity, the eigenchannels for the two transmission directions are plotted in the same panel; decoupled eigenchannels can be found in Figs. S1 and S4 of the SI.

well below and above the Fermi level, respectively. This result, together with those shown in Fig. 4 (and S1 of the SI) showing the coupling of the HOMO and LUMO eigenchannels with both electrodes (much higher in the case of the Ru electrode), point to a non-resonant transport

through the frontier orbitals. In the case of 4-aminophenyl, the coupling of the frontier orbitals of the molecule with the Gr/Ru electrode is much stronger, as shown in Fig. 4. But the transmission function exhibits a larger HOMO-LUMO gap (Fig. 3b) due to the smaller number of orbitals involved in its π-delocalization. The conjunction of these two effects leads to transport via a non-resonant coherent tunneling mechanism. Beyond the HOMO and LUMO peaks, in Fig. 3 we also observe a small peak at ~ -2 eV, which appears independently of the molecule or the anchoring position. This peak is strongly related to the overlap of the nitrogen lone pair with the Ru orbitals of the tip (see Fig. S2 of SI), and it is more pronounced in 4-aminophenyl because of the covalent nature of the bond between the molecule and graphene.

Another interesting feature that can be observed in Fig. 3, for both molecules, is the presence of a peak at -1.5 eV for the FCC-HCP anchoring position. This peak is due to localization of the electron density in between the graphene layer and Ru(0001) in the higher regions of the moiré, i.e., to the formation of a quantum dot as a consequence of the Gr/Ru decoupling in those regions [46]. This effect can be further confirmed by looking at S3 of the SI, where we have displayed the eigenchannel closest to −1.5 eV for both systems. From this figure, we can see that this eigenchannel extends all over the moiré hill. In the case of 4-aminophenyl this eigenchannel also extends over the molecule due to the covalent bond. Finally, for 4-aminophenyl, we can also observe a broad peak centered at -0.5 eV (see Fig. 3b), more pronounced for the FCC-HCP anchoring site, but with larger amplitude at the MID_1 site due to the larger delocalization of the electrons across the molecule/surface interphase. The presence of this peak can be attributed to hybridization between the molecule orbitals and the graphene bands. This hybridization phenomenon can be inferred from the shape of the eigenchannel at -0.5 eV shown in Fig. 4 bottom panel (and in S4 of the SI). This peak does not appear in the Gr/Ru-4-aminobenzonitrile-Ru transmission function because physisorption does not lead to orbital hybridization.

Although for each individual molecule the gross features of the transmission functions are very similar at the three anchoring sites, there are quantitative differences between the corresponding transmission values, which are at the origin of the strong modulation of the calculated currents and RRs with the anchoring site. From the analysis of the eigenchannel functions shown in Fig. 4 (and Fig. S1 in the SI), we observe that, for both molecules, there is a substantial overlap of the HOMO and LUMO frontier orbitals with those of the Ru top electrode irrespective of the anchoring site, which allows for zero-bias conductance. In contrast, none of the frontier orbitals of the 4-aminobenzonitrile overlap with those of the bottom Gr/Ru electrode at any anchoring position (except for the very weak interaction of the HOMO on the FCC-HCP site -see S1 of SI-). For 4-aminophenyl, we observe a different behavior. In this case, the interaction between the HOMO orbital of the molecule and graphene increases as the molecule approaches the HCP-TOP site. The LUMO orbital, on the other hand, significantly overlaps with the graphene orbitals, showing that for this molecule the zero-bias conductance is dominated by the LUMO.

Although at zero-bias there is no overlap between the frontier orbitals of 4-aminobenzonitrile and graphene at any of the studied anchoring sites, one can still overcome the energy barrier and reduce the energy gap by applying a positive bias, which improves the alignment of the Gr/Ru conduction bands with the molecular orbitals. This procedure enhances notably the conduction through a tunneling mechanism, as can be seen in Fig. 2a. This enhancement is particularly remarkable at the HCP-TOP anchoring site (the lower region of the moiré) due to a increase of the interaction between the molecule and the bottom Gr/Ru electrode, which is close to produce a true chemical bonding. When applying a negative bias, the energy levels of the tip bands that already had a significant overlap with the molecule's orbitals are shifted. As a result, the current increases due to the reduction of the potential barrier, but not as much as with a positive bias.

There is an interesting phenomenon observed at the FCC-HCP site for both molecules. Although the electron density on this site is large and the overlap between the molecule's orbitals and the graphene ones is favored, the current increases less at positive biases than in the other sites. At the FCC-HCP position, the distance between the graphene sheet and the Ru substrate is the largest in the moiré, and the electrons are localized in the quantum dot lying in between graphene and Ru. This reduces the overlap of the frontier orbitals with the Ru orbitals and makes electron tunneling more difficult. For both molecules at positive biases, a visual inspection of the molecule-Gr/Ru interaction in Fig. 4 (and Figs. S1, S2, S3 and S4 of the SI) indicates that the highest currents should be expected at the HCP-TOP site, followed by the MID_1 site, and then the FCC-HCP site for both molecules. However, 4-aminophenyl exhibits a different behavior. Although the interaction of this molecule with the lower electrode at the three anchoring sites varies following the previous criteria, a positive bias does not further improve the alignment of the 4-aminophenyl and Gr/Ru levels due to the covalent nature of the aniline-graphene interaction. The actual trend followed by the current can be understood by analyzing the interaction with the upper electrode (tip). Fig. 4 shows a slightly higher overlap at the MID_1 site over the HCP- TOP site in all the eigenchannels. Therefore, at positive bias, we would expect higher current-intensity at this position as evidenced in the I-V curve, Fig. 2b. On the other hand, the current can be notably enhanced by improving the alignment of the molecule's orbitals with the electrode states, i.e. improving the overlap with the tip. Therefore, when applying a negative bias, one can exploit all the states formed during the hybridization, previously discussed, and improve the tunneling mechanism. Finally, at negative bias the current has higher absolute values at the MID_1 position. To complement our hypothesis regarding the bias polarity we have computed the transmission function for both molecules, in Figs. 5 and 6, at −1.5 V and 1.5 V as a reference for negative and positive biases, respectively. And, to further support the analysis we have plotted their eigenchannels at the Fermi level in Figs. S7 and S8 of the SI. For both molecules, the results we have obtained are in complete agreement with our previous conclusions.

Aiming to understand whether the quantum dot present under the upper regions of the Gr/Ru moiré has a significant influence in the conductance of 4-aminobenzonitrile, taking into account the physisorption nature of its interaction with graphene, we have run simulations for the Gr/Ru-4-aminobenzonitrile-tip system for two extra anchoring sites, FCC-TOP (between HCP-TOP and MID_1) and MID_2 (between MID_1 and FCC-HCP) (see Fig.S5 of the SI). Interestingly, the transmission function (see Fig. S6a of the SI) at the MID_2 position shows a contribution of the quantum dot that can be seen at the same energy level as in FCC-HCP. However, the amplitude of this peak is insignificant and does not contribute to increase the current in comparison with the MID_1 site (see also Fig. S6b of the SI). At the FCC-TOP site, the effect is similar and the transmission function is alike to that at the HCP-TOP site, both without a significant contribution of the quantum dot.

4. Conclusions

In this work, we have shown, by means of fully atomistic DFT and transport calculations performed on 4-aminophenyl and 4-aminobenzonitrile, the potential of Gr/Ru electrodes to customize single-molecule conductivity. Thanks to their sizeable moiré pattern, which spatially modulates the geometric and electronic structure, the conductance can be modified by simply changing the anchoring site of the molecule within the electrode. We have found that, for the two investigated molecules, induced currents and rectification ratios are very different in the upper and lower anchoring positions of the moiré and that they can be monotonously varied by gradually moving the molecules from the former to the latter position. The variations in the currents can be as large as an order of magnitude, and up to a factor of 5 in the rectification ratios. These differences can also be modulated at

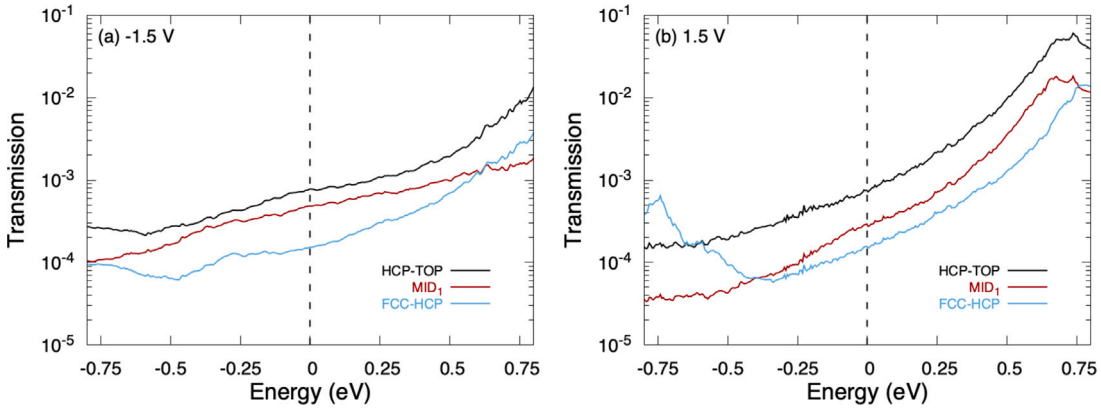

Fig. 5. Non-equilibrium transmission functions at (a) −1.5 V and (b) 1.5 V at positions shown in Fig. 1 using 4-aminobenzonitrile as single-molecule junction. Dashed black lines indicate to the Fermi level.

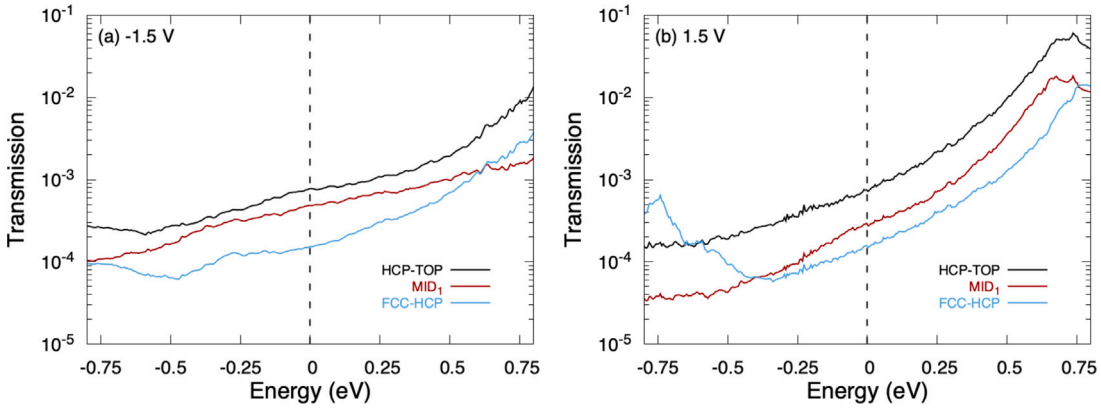

Fig. 6. Non-equilibrium transmission functions at (a) −1.5 V and (b) 1.5 V at positions shown in Fig. 1 using 4-aminophenyl as single-molecule junction. Dashed black lines indicate to the Fermi level.

will by just varying the bias voltage. For bias voltages where differences in the electric current are more pronounced, 4-aminophenyl and 4-aminobenzonitrile behave quite differently: for 4-aminobenzonitrile, the largest current values are obtained for molecules anchored on the lower areas of the moiré, while for 4-aminophenyl the largest value is obtained on the intermediate areas. This is due to the very different nature of the chemical bond between the molecule and the Gr/Ru substrate: covalent for 4-aminophenyl and dispersive for 4-aminobenzonitrile (physisorption). At the highest regions of the moiré, conductance has been found to be nearly independent of the nature of the molecule-Gr/Ru bonding. In this case, both molecules experience a reduction in their transport properties due to the weak coupling with the Gr/Ru electrode. In summary, our results show that Gr/Ru is indeed a very promising system to tailor single-molecule conductivity under the experimental conditions commonly found in nowadays laboratories. We expect that the present study will encourage additional experimental and theoretical measurements for its implementation as usual electrode in molecular electronics.

CRediT authorship contribution statement

Joel G. Fallaque: Software, Formal analysis, Investigation, Writing – original draft. **Sandra Rodríguez-González:** Methodology, Formal analysis, Investigation, Writing – original draft. **Cristina Díaz:** Conceptualization, Resources, Writing – original draft, Supervision, Funding acquisition. **Fernando Martín:** Conceptualization, Resources, Writing – review & editing, Supervision, Funding acquisition.

Declaration of competing interest

The authors declare that they have no known competing financial interests or personal relationships that could have appeared to influence the work reported in this paper.

Data availability

Data will be made available on request.

Acknowledgments

This work was supported by the Spanish Ministry of Science and Innovation – Ministerio Español de Ciencia e Innovación MICINN – projects PID2019-105458RB-I00, PID2019-106732GB-I00, the Severo Ochoa Programme for Centres of Excellence in R &D (SEV-2016-0686) and the María de Maeztu Programme for Units of Excellence in R &D (CEX2018-000805-M). We acknowledge the generous allocation of computer time at the Barcelona Supercomputer Center and the Centro de Computación Científica at the Universidad Autónoma de Madrid (CCC-UAM).

Appendix A. Supplementary data

Supplementary material related to this article can be found online at https://doi.org/10.1016/j.apsusc.2023.158943.

References

[1] A. Aviram, M.A. Ratner, Molecular rectifiers, Chem. Phys. Lett. 29 (2) (1974) 277–283, http://dx.doi.org/10.1016/0009-2614(74)85031-1.

[2] L. Sun, Y.A. Diaz-Fernandez, T.A. Gschneidtner, F. Westerlund, S. Lara-Avila, K. Moth-Poulsen, Single-molecule electronics: from chemical design to functional devices, Chem. Soc. Rev. 43 (2014) 7378–7411, http://dx.doi.org/10.1039/C4CS00143E.

[3] E. Leary, A. La Rosa, M.T. González, G. Rubio-Bollinger, N. Agraït, N. Martín, Incorporating single molecules into electrical circuits. The role of the chemical anchoring group, Chem. Soc. Rev. 44 (2015) 920–942, http://dx.doi.org/10.1039/C4CS00264D.

[4] M.A. Reed, C. Zhou, C.J. Muller, T.P. Burgin, J.M. Tour, Conductance of a molecular junction, Science 278 (5336) (1997) 252–254, http://dx.doi.org/10.1126/science.278.5336.252.

[5] F. Chen, N.J. Tao, Electron transport in single molecules: From benzene to graphene, Acc. Chem. Res. 42 (3) (2009) 429–438, http://dx.doi.org/10.1021/ar800199a.

[6] S.Y. Sayed, J.A. Fereiro, H. Yan, R.L. McCreery, A.J. Bergren, Charge transport in molecular electronic junctions: Compression of the molecular tunnel barrier in the strong coupling regime, Proc. Natl. Acad. Sci. 109 (29) (2012) 11498–11503, http://dx.doi.org/10.1073/pnas.1201557109.

[7] C. Huang, A.V. Rudnev, W. Hong, T. Wandlowski, Break junction under electrochemical gating: testbed for single-molecule electronics, Chem. Soc. Rev. 44 (2015) 889–901, http://dx.doi.org/10.1039/C4CS00242C.

[8] A.J. Bergren, R.L. McCreery, S.R. Stoyanov, S. Gusarov, A. Kovalenko, Electronic characteristics and charge transport mechanisms for large area aromatic molecular junctions, J. Phys. Chem. C 114 (37) (2010) 15806–15815, http://dx.doi.org/10.1021/jp106362q.

[9] F. Anariba, R.L. McCreery, Electronic conductance behavior of carbon-based molecular junctions with conjugated structures, J. Phys. Chem. B 106 (40) (2002) 10355–10362, http://dx.doi.org/10.1021/jp026285e.

[10] R.L. McCreery, H. Yan, A.J. Bergren, A critical perspective on molecular electronic junctions: there is plenty of room in the middle, Phys. Chem. Chem. Phys. 15 (2013) 1065–1081, http://dx.doi.org/10.1039/C2CP43516K.

[11] F. Chen, X. Li, J. Hihath, Z. Huang, N. Tao, Effect of anchoring groups on single-molecule conductance: comparative study of thiol-, amine-, and carboxylic-acid-terminated molecules, J. Am. Chem. Soc. 128 (49) (2006) 15874–15881, http://dx.doi.org/10.1021/ja065864k.

[12] P. Moreno-García, M. Gulcur, D.Z. Manrique, T. Pope, W. Hong, V. Kaliginedi, C. Huang, A.S. Batsanov, M.R. Bryce, C. Lambert, T. Wandlowski, Single-molecule conductance of functionalized oligoynes: Length dependence and junction evolution, J. Am. Chem. Soc. 135 (33) (2013) 12228–12240, http://dx.doi.org/10.1021/ja4015293.

[13] Q. Zhang, L. Liu, S. Tao, C. Wang, C. Zhao, C. González, Y.J. Dappe, R.J. Nichols, L. Yang, Graphene as a promising electrode for low-current attenuation in nonsymmetric molecular junctions, Nano Lett. 16 (10) (2016) 6534–6540, http://dx.doi.org/10.1021/acs.nanolett.6b03180.

[14] Q. Zhang, S. Tao, R. Yi, C. He, C. Zhao, W. Su, A. Smogunov, Y.J. Dappe, R.J. Nichols, L. Yang, Symmetry effects on attenuation factors in graphene-based molecular junctions, J. Phys. Chem. Lett. 8 (24) (2017) 5987–5992, http://dx.doi.org/10.1021/acs.jpclett.7b02822.

[15] S. Rodríguez-González, Z. Xie, O. Galangau, P. Selvanathan, L. Norel, C. Van Dyck, K. Costuas, C.D. Frisbie, S. Rigaut, J. Cornil, HOMO level pinning in molecular junctions: Joint theoretical and experimental evidence, J. Phys. Chem. Lett. 9 (9) (2018) 2394–2403, http://dx.doi.org/10.1021/acs.jpclett.8b00575.

[16] M.-J. Huang, L.-Y. Hsu, M.-D. Fu, S.-T. Chuang, F.-W. Tien, C.-h. Chen, Conductance of tailored molecular segments: A rudimentary assessment by Landauer formulation, J. Am. Chem. Soc. 136 (5) (2014) 1832–1841, http://dx.doi.org/10.1021/ja4088538.

[17] W. Hong, D.Z. Manrique, P. Moreno-García, M. Gulcur, A. Mishchenko, C.J. Lambert, M.R. Bryce, T. Wandlowski, Single molecular conductance of tolanes: Experimental and theoretical study on the junction evolution dependent on the anchoring group, J. Am. Chem. Soc. 134 (4) (2012) 2292–2304, http://dx.doi.org/10.1021/ja209844r.

[18] E. Lörtscher, C.J. Cho, M. Mayor, M. Tschudy, C. Rettner, H. Riel, Influence of the anchor group on charge transport through single-molecule junctions, ChemPhysChem 12 (9) (2011) 1677–1682, http://dx.doi.org/10.1002/cphc.201000960.

[19] C.R. Arroyo, E. Leary, A. Castellanos-Gómez, G. Rubio-Bollinger, M.T. González, N. Agraït, Influence of binding groups on molecular junction formation, J. Am. Chem. Soc. 133 (36) (2011) 14313–14319, http://dx.doi.org/10.1021/ja201861k.

[20] M. Kiguchi, H. Nakamura, Y. Takahashi, T. Takahashi, T. Ohto, Effect of anchoring group position on formation and conductance of a single disubstituted benzene molecule bridging Au electrodes: Change of conductive molecular orbital and electron pathway, J. Phys. Chem. C 114 (50) (2010) 22254–22261, http://dx.doi.org/10.1021/jp1095079.

[21] B. Limburg, J.O. Thomas, G. Holloway, H. Sadeghi, S. Sangtarash, I.C.-Y. Hou, J. Cremers, A. Narita, K. Müllen, C.J. Lambert, G.A.D. Briggs, J.A. Mol, H.L. Anderson, Anchor groups for graphene-porphyrin single-molecule transistors, Adv. Funct. Mater. 28 (45) (2018) 1803629, http://dx.doi.org/10.1002/adfm.201803629.

[22] H. Sadeghi, S. Sangtarash, C. Lambert, Robust molecular anchoring to graphene electrodes, Nano Lett. 17 (8) (2017) 4611–4618, http://dx.doi.org/10.1021/acs.nanolett.7b01001.

[23] J. Chen, L. Calvet, M. Reed, D. Carr, D. Grubisha, D. Bennett, Electronic transport through metal–1,4-phenylene diisocyanide–metal junctions, Chem. Phys. Lett. 313 (5) (1999) 741–748, http://dx.doi.org/10.1016/S0009-2614(99)01060-X.

[24] J.M. Seminario, C.E. De La Cruz, P.A. Derosa, A theoretical analysis of metal–molecule contacts, J. Am. Chem. Soc. 123 (23) (2001) 5616–5617, http://dx.doi.org/10.1021/ja015661q.

[25] C.-H. Ko, M.-J. Huang, M.-D. Fu, C.-h. Chen, Superior contact for single-molecule conductance: Electronic coupling of thiolate and isothiocyanate on Pt, Pd, and Au, J. Am. Chem. Soc. 132 (2) (2010) 756–764, http://dx.doi.org/10.1021/ja9084012.

[26] J.W. Lawson, C.W. Bauschlicher, Transport in molecular junctions with different metallic contacts, Phys. Rev. B 74 (2006) 125401, http://dx.doi.org/10.1103/PhysRevB.74.125401.

[27] T. Kim, H. Vázquez, M.S. Hybertsen, L. Venkataraman, Conductance of molecular junctions formed with silver electrodes, Nano Lett. 13 (7) (2013) 3358–3364, http://dx.doi.org/10.1021/nl401654s.

[28] T. Nakazumi, S. Kaneko, M. Kiguchi, Electron transport properties of Au, Ag, and Cu atomic contacts in a hydrogen environment, J. Phys. Chem. C 118 (14) (2014) 7489–7493, http://dx.doi.org/10.1021/jp5012318.

[29] S. Ranganathan, I. Steidel, F. Anariba, R.L. McCreery, Covalently bonded organic monolayers on a carbon substrate: a new paradigm for molecular electronics, Nano Lett. 1 (9) (2001) 491–494, http://dx.doi.org/10.1021/nl015566f.

[30] A.J. Bergren, K.D. Harris, F. Deng, R.L. McCreery, Molecular electronics using diazonium-derived adlayers on carbon with cu top contacts: critical analysis of metal oxides and filaments, J. Phys.: Condens. Matter 20 (37) (2008) 374117, http://dx.doi.org/10.1088/0953-8984/20/37/374117.

[31] A.V. Rudnev, V. Kaliginedi, A. Droghetti, H. Ozawa, A. Kuzume, M. aki Haga, P. Broekmann, I. Rungger, Stable anchoring chemistry for room temperature charge transport through graphite-molecule contacts, Sci. Adv. 3 (6) (2017) e1602297, http://dx.doi.org/10.1126/sciadv.1602297.

[32] A. Castellanos-Gomez, S. Bilan, L.A. Zotti, C.R. Arroyo, N. Agraït, J. Carlos Cuevas, G. Rubio-Bollinger, Carbon tips as electrodes for single-molecule junctions, Appl. Phys. Lett. 99 (12) (2011) 123105, http://dx.doi.org/10.1063/1.3643031.

[33] L. Liu, Q. Zhang, S. Tao, C. Zhao, E. Almutib, Q. Al-Galiby, S.W.D. Bailey, I. Grace, C.J. Lambert, J. Du, L. Yang, Charge transport through dicarboxylic-acid-terminated alkanes bound to graphene–gold nanogap electrodes, Nanoscale 8 (2016) 14507–14513, http://dx.doi.org/10.1039/C6NR03807G.

[34] S. Tao, Q. Zhang, A. Vezzoli, C. Zhao, C. Zhao, S.J. Higgins, A. Smogunov, Y.J. Dappe, R.J. Nichols, L. Yang, Electrochemical gating for single-molecule electronics with hybrid au|graphene contacts, Phys. Chem. Chem. Phys. 24 (2022) 6836–6844, http://dx.doi.org/10.1039/D1CP05486D.

[35] R. McCreery, J. Dieringer, A.O. Solak, B. Snyder, A.M. Nowak, W.R. McGovern, S. DuVall, Molecular rectification and conductance switching in carbon-based molecular junctions by structural rearrangement accompanying electron injection, J. Am. Chem. Soc. 125 (35) (2003) 10748–10758, http://dx.doi.org/10.1021/ja0362196.

[36] T. Kim, Z.-F. Liu, C. Lee, J.B. Neaton, L. Venkataraman, Charge transport and rectification in molecular junctions formed with carbon-based electrodes, Proc. Natl. Acad. Sci. 111 (30) (2014) 10928–10932, http://dx.doi.org/10.1073/pnas.1406926111.

[37] C. Díaz, F. Calleja, A.L. Vázquez de Parga, F. Martín, Graphene grown on transition metal substrates: Versatile templates for organic molecules with new properties and structures, Surf. Sci. Rep. 77 (4) (2022) 100575, http://dx.doi.org/10.1016/j.surfrep.2022.100575.

[38] F. Prins, A. Barreiro, J.W. Ruitenberg, J.S. Seldenthuis, N. Aliaga-Alcalde, L.M.K. Vandersypen, H.S.J. van der Zant, Room-temperature gating of molecular junctions using few-layer graphene nanogap electrodes, Nano Lett. 11 (11) (2011) 4607–4611, http://dx.doi.org/10.1021/nl202065x.

[39] V.M. García-Suárez, R. Ferradás, D. Carrascal, J. Ferrer, Universality in the low-voltage transport response of molecular wires physisorbed onto graphene electrodes, Phys. Rev. B 87 (2013) 235425, http://dx.doi.org/10.1103/PhysRevB.87.235425.

[40] J.A. Mol, C.S. Lau, W.J.M. Lewis, H. Sadeghi, C. Roche, A. Cnossen, J.H. Warner, C.J. Lambert, H.L. Anderson, G.A.D. Briggs, Graphene-porphyrin single-molecule transistors, Nanoscale 7 (2015) 13181–13185, http://dx.doi.org/10.1039/C5NR03294F.

[41] F. Hüser, G.C. Solomon, Electron transport in molecular junctions with graphene as protecting layer, J. Chem. Phys. 143 (21) (2015) 214302, http://dx.doi.org/10.1063/1.4936409.

[42] P. Song, C.S.S. Sangeeth, D. Thompson, W. Du, K.P. Loh, C.A. Nijhuis, Noncovalent self-assembled monolayers on graphene as a highly stable platform for molecular tunnel junctions, Adv. Mater. 28 (4) (2016) 631–639, http://dx.doi.org/10.1002/adma.201504207.

[43] W. Moritz, B. Wang, M.-L. Bocquet, T. Brugger, T. Greber, J. Wintterlin, S. Günther, Structure determination of the coincidence phase of graphene on Ru(0001), Phys. Rev. Lett. 104 (2010) 136102, http://dx.doi.org/10.1103/PhysRevLett.104.136102.

[44] D. Martoccia, M. Björck, C.M. Schlepütz, T. Brugger, S.A. Pauli, B.D. Patterson, T. Greber, P.R. Willmott, Graphene on Ru(0001): a corrugated and chiral structure, New J. Phys. 12 (4) (2010) 043028, http://dx.doi.org/10.1088/1367-2630/12/4/043028.

[45] A.L. Vázquez de Parga, F. Calleja, B. Borca, M.C.G. Passeggi, J.J. Hinarejos, F. Guinea, R. Miranda, Periodically rippled graphene: Growth and spatially resolved electronic structure, Phys. Rev. Lett. 100 (2008) 056807, http://dx.doi.org/10.1103/PhysRevLett.100.056807.

[46] D. Stradi, S. Barja, C. Díaz, M. Garnica, B. Borca, J.J. Hinarejos, D. Sánchez-Portal, M. Alcamí, A. Arnau, A.L. Vázquez de Parga, R. Miranda, F. Martín, Role of dispersion forces in the structure of graphene monolayers on Ru surfaces, Phys. Rev. Lett. 106 (2011) 186102, http://dx.doi.org/10.1103/PhysRevLett.106.186102.

[47] D. Stradi, S. Barja, C. Díaz, M. Garnica, B. Borca, J.J. Hinarejos, D. Sánchez-Portal, M. Alcamí, A. Arnau, A.L. Vázquez de Parga, R. Miranda, F. Martín, Electron localization in epitaxial graphene on Ru(0001) determined by moiré corrugation, Phys. Rev. B 85 (2012) 121404, http://dx.doi.org/10.1103/PhysRevB.85.121404.

[48] J.J. Navarro, M. Pisarra, B. Nieto-Ortega, J. Villalva, C.G. Ayani, C. Díaz, F. Calleja, R. Miranda, F. Martín, E.M. Pérez, A.L.V. de Parga, Graphene catalyzes the reversible formation of a C–C bond between two molecules, Sci. Adv. 4 (12) (2018) eaau9366, http://dx.doi.org/10.1126/sciadv.aau9366.

[49] D. Stradi, M. Garnica, C. Díaz, F. Calleja, S. Barja, N. Martín, M. Alcamí, A.L. Vázquez de Parga, R. Miranda, F. Martín, Controlling the spatial arrangement of organic magnetic anions adsorbed on epitaxial graphene on Ru(0001), Nanoscale 6 (2014) 15271–15279, http://dx.doi.org/10.1039/C4NR02917H.

[50] M. Garnica, D. Stradi, F. Calleja, S. Barja, C. Díaz, M. Alcamí, A. Arnau, A.L. Vázquez de Parga, F. Martín, R. Miranda, Probing the site-dependent kondo response of nanostructured graphene with organic molecules, Nano Lett. 14 (8) (2014) 4560–4567, http://dx.doi.org/10.1021/nl501584v.

[51] M. Garnica, D. Stradi, S. Barja, F. Calleja, C. Díaz, M. Alcamí, N. Martín, A.L. Vázquez de Parga, F. Martín, R. Miranda, Long-range magnetic order in a purely organic 2D layer adsorbed on epitaxial graphene, Nat. Phys. 9 (2013) 368, http://dx.doi.org/10.1038/NPHYS2610.

[52] Z. Tehrani, H.Y. Abbasi, A. Devadoss, J.E. Evans, O.J. Guy, Assessing surface coverage of aminophenyl bonding sites on diazotised glassy carbon electrodes for optimised electrochemical biosensor performance, Nanomaterials 11 (2) (2021) http://dx.doi.org/10.3390/nano11020416.

[53] G. Ambrosio, G. Drera, G.D. Santo, L. Petaccia, L. Daukiya, A. Brown, B. Hirsch, S.D. Feyter, L. Sangaletti, S. Pagliara, Interface chemistry of graphene/Cu grafted by 3,4,5-tri-methoxyphenyl, Sci. Rep. 10 (2020) 4114, http://dx.doi.org/10.1038/s41598-020-60831-8.

[54] G. Kresse, J. Furthmüller, Efficient iterative schemes for ab initio total-energy calculations using a plane-wave basis set, Phys. Rev. B 54 (1996) 11169–11186, http://dx.doi.org/10.1103/PhysRevB.54.11169.

[55] J.P. Perdew, K. Burke, M. Ernzerhof, Generalized gradient approximation made simple, Phys. Rev. Lett. 77 (1996) 3865–3868, http://dx.doi.org/10.1103/PhysRevLett.77.3865.

[56] A. Tkatchenko, M. Scheffler, Accurate molecular Van Der Waals interactions from ground-state electron density and free-atom reference data, Phys. Rev. Lett. 102 (2009) 073005, http://dx.doi.org/10.1103/PhysRevLett.102.073005.

[57] G. Kresse, D. Joubert, From ultrasoft pseudopotentials to the projector augmented-wave method, Phys. Rev. B 59 (1999) 1758–1775, http://dx.doi.org/10.1103/PhysRevB.59.1758.

[58] N. Papior, N. Lorente, T. Frederiksen, A. García, M. Brandbyge, Improvements on non-equilibrium and transport Green function techniques: The next-generation transiesta, Comput. Phys. Comm. 212 (2017) 8–24, http://dx.doi.org/10.1016/j.cpc.2016.09.022.

[59] M. Leijnse, W. Sun, M.B. Nielsen, P. Hedegård, K. Flensberg, Interaction-induced negative differential resistance in asymmetric molecular junctions, J. Chem. Phys. 134 (10) (2011) 104107, http://dx.doi.org/10.1063/1.3560474.

[60] K. Wang, J. Zhou, J.M. Hamill, B. Xu, Measurement and understanding of single-molecule break junction rectification caused by asymmetric contacts, J. Chem. Phys. 141 (5) (2014) 054712, http://dx.doi.org/10.1063/1.4891862.

[61] T.H. Kim, J. Lee, R.-G. Lee, Y.-H. Kim, Gate- versus defect-induced voltage drop and negative differential resistance in vertical graphene heterostructures, NPJ Comput. Mater. 8 (1) (2022) 50, http://dx.doi.org/10.1038/s41524-022-00731-9.